e-Polymers **2006**, no. 072

http://www.e-polymers.org
ISSN 1618-7229

One-pot synthesis of PMMA/montmorillonite nanocomposites

Adam Kiersnowski[*]*, Maria Trelinska-Wlazlak, Justyna Dolega and Jacek Piglowski*

Polymer Engineering & Technology Division, Wroclaw University of Technology, Wybrzeze Wyspianskiego 27, 50-370 Wroclaw, Poland
*Adam Kiersnowski, Tel. +48 71 320 2814, E-Mail: adam.kiersnowski@pwr.wroc.pl
Maria Trelinska-Wlazlak: Tel. +48 71 320 2467, E-Mail: trelinska@interia.pl
Justyna Dolega: Tel. +48 71 320 2814, E-Mail: justyna.dolega@pwr.wroc.pl
Jacek Piglowski: group head, Tel. +48 71 320 3510, E-Mail: jacek.piglowski@pwr.wroc.pl

(Received: 4 May, 2006; published: 14 November, 2006)

***Abstract*:** This article describes simple preparation methods of poly(methyl methacrylate) (PMMA)/synthetic montmorillonite nanocomposites by single-step *in situ* polymerizations. Compatibility between PMMA and the silicate was ensured by an addition of (3-acrylamidepropyl) trimethylammonium chloride (AAPTMA). The work also compares how different synthetic routes, namely emulsion and solution polymerization, affect the structure as well as thermal and mechanical properties of obtained nanocomposites. The results of structural investigations clearly show, that both the techniques lead to intercalated nanocomposites, but emulsion polymerization allows more effective deflocculating and intercalating of the clay with acrylic copolymers. The addition of small amounts of layered silicates causes an increase in thermal stability and stiffness of the materials. It is demonstrated that at 5 wt. % of the filler, the temperature of 10 % weight loss was shifted up by nearly 50 K in comparison to the neat PMMA. In the same sample, the Young's modulus of the material was found to be increased by 26 %.
Keywords: PMMA, polymer-clay nanocomposites, synthesis, structure, properties

Introduction

An important point in the developing of engineering polymers is to reinforce the polymer matrix and improve strength, stiffness, thermal stability or barrier properties without sacrificing good processability, toughness and optical properties. In conventional composites with macroscopically separated phases, the property enhancement is achieved at 30 - 40 weight percent of filler, which often causes serious increase in density of the material. An alternative now is polymer-clay nanocomposites where improvements in properties are observed at few weight percent of the filler, that allows retaining the density of the resin at low level.[1, 2]

It should be emphasized here, that not all polymer-clay systems are nanocomposites. When polymer is unable to penetrate the silicate particles i.e. it is unable to intercalate between the clay layers, a conventional, phase separated composite is formed. Such systems are usually referred to as microcomposites. The materials are considered as nanocomposites exclusively in cases where the polymer and the mineral are integrated at the nanoscale. Then, depending on the structure of the silicate particles dispersed throughout the polymer matrix, nanocomposites can be classed into two main groups: intercalated or exfoliated (delaminated) systems. In the first case, the characteristic periodic, multilayer structure of the clay is retained after intercalation of polymer inside the galleries. However, due to insertion of

macromolecules, the gap between individual layers (defined by a distance between (001) crystallographic planes – d_{001}) within a single silicate stack is increased in comparison to initial value. In exfoliated nanocomposites, all clay particles are disintegrated into discrete platelets, with diameter of approximately 100-200 nm and 1 nm in thickness, uniformly distributed in the polymer. In practice, the volume fractions of the clay introduced in the matrices of exfoliated nanocomposites are slightly lower then in intercalated systems. [1,2]

One of the main reasons why formation of nanocomposites is not that easy is the fact that particles of layered silicates in a pristine state are well dispersible only in hydrophilic polymers such as poly(vinyl alcohol) or poly(ethylene oxide) [3]. Therefore, typically one has to pass through a stepwise procedure of compatibilization of the silicate and the polymer followed by formation of the nanocomposite. Before the layered clay can be added to a polymer or monomer, it should be rendered hydrophobic (organophilic) so that it could form stable dispersions in the organic continuous phase. To achieve that, the alkali metal ions (such as Na^+) residing inside the interlayer spaces must be exchanged with e.g. amphiphilic alkylammonium salts. [1, 2, 4] With organophilic layered silicate, three different ways to synthesize polymer-clay nanocomposites are possible: melt intercalation, solution blending and *in situ* intercalative polymerization. [5-9] The main disadvantage of the above mentioned pathways is that the nanocomposites are obtained in multi-stage processes involving clay modification, followed by drying, and milling the organoclay that can be finally introduced and dispersed in the polymer bulk.

Irrespective of the method of formation, the compatibility between the filler and the polymer plays a key role. For example, polypropylene-clay systems are compatible, when polymer matrix is modified by addition of polypropylene grafted with maleic anhydride or by application of diamines as clay modifier. [10, 11] The compatibility between layered silicates with styrene and methyl methacrylate may be improved by adding ammonium-functionalized styrene, ammonium-modified methacrylate, or copolymers containing pendant ammonium groups. [12, 13] As it is clearly shown in cited references, it is very difficult to obtain nanocomposites of incompatible substrates, and even if one succeeds, the materials usually reveal inferior properties.

Here we discuss the structure as well as thermal and mechanical properties of poly(methyl methacrylate)-montmorillonite nanocomposites obtained by emulsion and solution polymerizations. The main advantage of presented routes over those typically applied is that the nanocomposites were synthesized out of raw substrates during single processes. Compatibility between system components was ensured by an addition of (3-acrylamidepropyl) trimethylammonium chloride (AAPTMA) which is capable of attaching to the clay surface through ionic interactions. On the other hand, AAPTMA is miscible and copolymerizable with methyl methacrylate. Due to its amphiphilicity, the compound was believed to locate at the PMMA/silicate interface. Similar method of compatibilization was described by Ciardelli and coworkers in their pioneering work. [14] Unlike the reported method, where montmorillonite after the ion-exchange with quaternized ammonium-acrylic monomers was filtered; vacuum-dried and milled, in our case the monomer was mixed with the organophilized montmorillonite directly after ion-exchange i.e. with a slurry (suspension) of the clay – thus the term ‘one pot’ in the title. We believe that, at the industrial scale, elimination of drying and milling processes may positively impact economic aspects of production of the nanocomposites as well as shorten the time of synthesis.

Results and discussion

Nanocomposites were investigated by classical X-ray diffraction method and scanning electron microscopy in order to determine the influence of synthetic route on layered structure and distribution of clay particles embedded in polymer matrix. XRD curves recorded for all the materials within 2 theta range of 1-10° are shown in Fig. 1a and 1b.

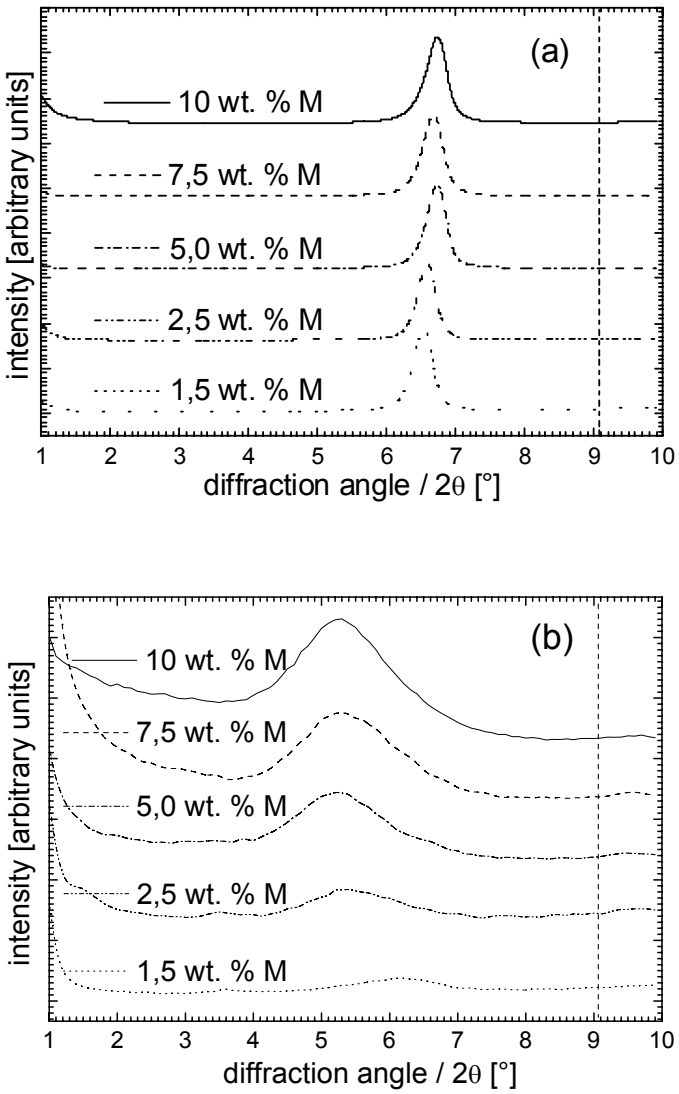

Fig. 1. XRD traces recorded for solution-polymerized (a) and emulsion-polymerized (b) acrylic nanocomposites. Vertical dashed lines in the figures indicate the initial position of diffraction maximum recorded for neat montmorillonite.

In all samples under investigation, the formation of intercalated nanocomposites was evidenced by the shift of basal 001 reflection towards lower angles which, according to the Bragg's law, indicates an increase in the interlayer distance (d_{001}) of montmorillonite. It can be easily noticed that diffraction patterns obtained for solvent- and emulsion- polymerized samples significantly differ from each other. In the case of nanocomposites obtained *via* solution polymerization, the scattering peaks are sharp and distinct. The value of interlayer spacing (d_{001}) of montmorillonite in these

samples is 1,33 nm and they are practically independent of the clay loading. The average reflection width is 4,7 mrad (±0,51 mrad) which means that the average thickness of the single clay crystallite, calculated using Scherrer equation, approximates 30 nm. Interlayer distances (d_{001}) in emulsion-polymerized samples are slightly higher and they are approximately 1,6 nm. The diffraction maxima recorded for these materials are considerably broader (22 mrad ±1,42 mrad; Fig. 1b) which may be a result of certain spread of d_{001} distances within clay tactoids as well as a decrease in number of clay layers within stacks. The average thickness of crystallites, calculated from peak breadths, is about 7 nm, which indicates that single tactoid is composed of roughly four layers.

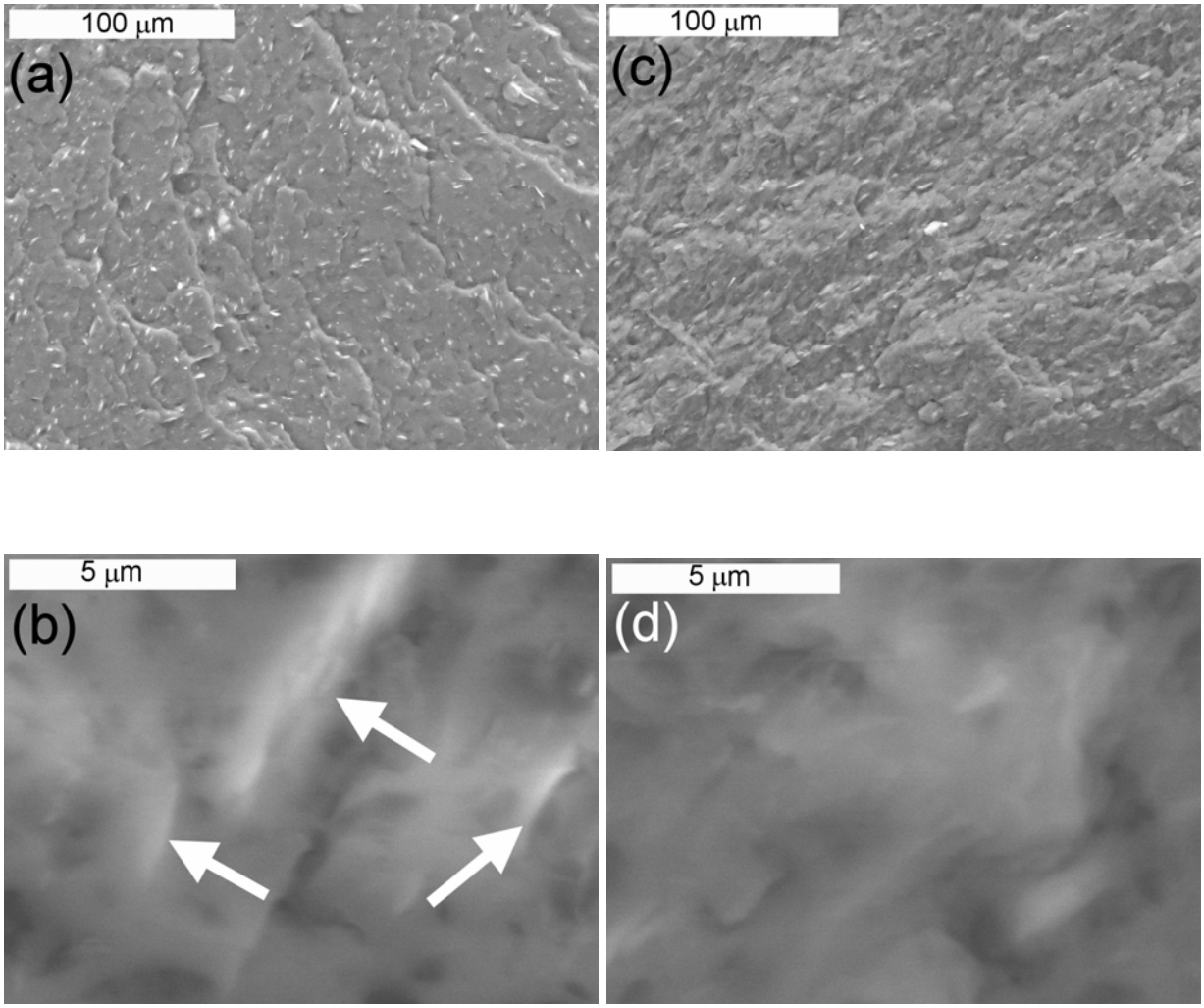

Fig. 2. Typical SEM micrographs (with phase contrast) of the solution ((a) and (b), to the left) and emulsion-polymerized nanocomposites ((c) and (d), to the right). Bars indicate 100 or 5 microns in upper and lower pictures respectively. Arrows in figure (b) tick silicate-rich areas.

Images from scanning electron microscope, recorded for samples co(S)-2,2/M 95/5 and co(E)-2,2/M 95/5 (fig. 2 a-d) were taken in order to estimate the dimensions of clay particles embedded in the resin. In the pictures, primary particles of the silicate can be seen as bright strands uniformly distributed in gray background (polymeric

matrix). At a glance one can see that in the sample obtained from solvent polymerization (co(S)-2,2/M 95/5 – figure 2 a and b), the silicate particles create micron-sized clusters while in the 'emulsion' nanocomposite (figure 2 c and d) they are hardly visible, even at higher magnifications (figure 2 b and d). These observations perfectly support the results obtained by means of X-ray diffraction method. Emulsion polymerization of the acrylic monomers leads to formation of intercalated nanocomposites in which the average thickness of tactoids is very low. The materials obtained by polymerization in solution are intercalated nanocomposites as well, but mean size of particles in this case is substantially larger.

Comparing the results of structural studies, one can conclude that the emulsion polymerization is more effective method for deflocculating and intercalating the montmorillonite than the process in solvent. In the nanocomposites synthesized by solvent polymerization, well-ordered, layered structure of the clay is retained even after intercalation of copolymer and the mean sizes of clay particles are considerably larger. On the contrary, in emulsion-polymerized materials, incorporation of polymer into interlayer spaces of montmorillonite causes desirable disordering in clay particles causing significant thinning of the tactoids.

Thermal properties of acrylic nanocomposites were studied by classical thermoanalytical techniques, namely thermogravimetry (TG) and differential scanning calorimetry (DSC). The investigations were aimed at gaining an insight into how the synthesis method and thus the structure, affect thermal stability (TG) and glass transition temperature (DSC) of copolymer in nanocomposites. Figure 3 shows TG curves measured for representative samples: co(S)-2,2/M 95/5 and co(E)-2,2/M 95/5. The temperature of 10 % weight loss (T_{10}), which has been chosen as a criterion for thermal stability, is marked in the figure with vertical, dotted lines. As it can be seen, the thermal stability of pure PMMA is the lowest and the T_{10} value is of 225°C. Both the nanocomposites were more stable; T_{10} temperatures recorded for co(S)-2,2/M 95/5 and co(E)-2,2/M 95/5 were 243 and 274 °C respectively.

In an attempt to explain the differences observed in thermal stabilities of acrylic nanocomposites, one should consider the results of structural studies. Intercalated clay particles embedded in the emulsion- or solvent-polymerized matrices are of different thicknesses. They consist of approx. 20 – 22 crystalline platelets in co(S) samples and roughly 4 platelets in co(E) nanocomposites, which means that, at the same volume fraction of silicate in the material, there is more individual particles in emulsion-polymerized samples. As it is known from the literature, superior thermal stability of nanocomposites is due to the formation of the maze of oblate montmorillonite particles that hinder mass transport within the material and therefore retard evolving of the volatile products. [1] A logical consequence of larger number of clay particles in the material is more tortuous path for gaseous products of thermal decomposition and thus improved thermostability. Our results are in accordance with this reasoning – better thermal stability of obtained acrylic nanocomposites is achieved in emulsion-polymerized composites, where primary montmorillonite tactoids are separated into larger number of thinner particles. Additionally, the results clearly show that complete exfoliation of montmorillonite is not a necessary condition for enhancement of thermal properties of nanocomposites, as suggested in previous literature reports. [15]

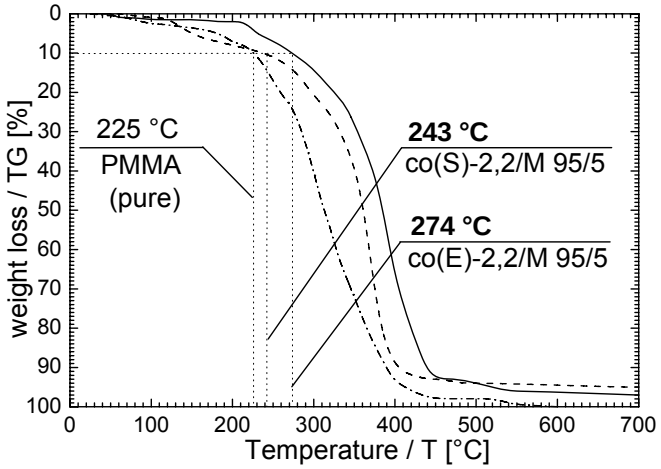

Fig. 3. TG curves of pure poly(methyl methacrylate) and the nanocomposites containing 5 wt. % of the clay.

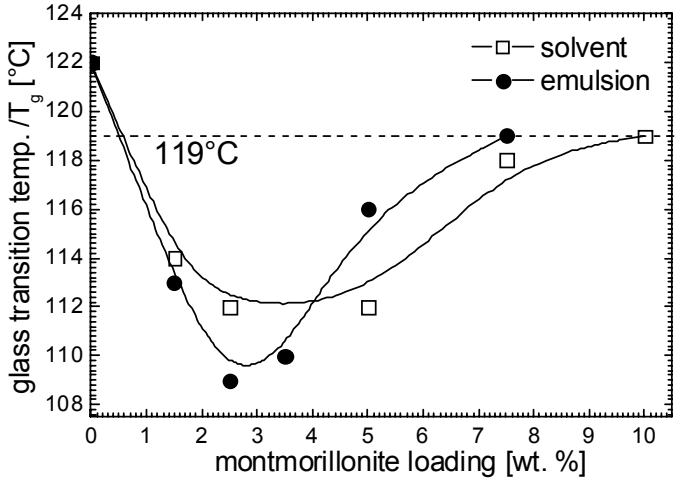

Fig. 4. Glass transition temperatures (T_g) of the nanocomposites as a function of silicate content. Hollow squares (□) denote the materials obtained by solution polymerization while solid circles (●) indicate "emulsion" nanocomposites.

An influence of filler content on glass transition temperature (T_g) was studied by differential scanning calorimetry. All T_g-values recorded for composites and pure PMMA are shown in Fig. 4. The curves of T_g vs. clay content obtained from analysis of emulsion- and solvent polymerized materials are similar – both have a minimum at silicate loading of 3 wt. % approximately, followed by gradual increase in T_g, to 119°C. One should note here that T_g in the obtained nanocomposites is affected by increasing content of two components (cf. Tab. 1) namely AAPTMA and montmorillonite. Polymerization of the neat AAPTMA leads to a rubbery polymer which has low glass transition temperature; thus the higher the mole ratio of AAPTMA in copolymer, the lower T_g. On the other hand, it is known, that presence of montmorillonite triggers an increase in T_g of acrylic nanocomposites. [16]

Consequently, at relatively low silicate content, AAPTMA seems to play a dominant role and therefore gradual drop in T_g is observed. Above a certain threshold loading of the clay (3 wt. % approx.), glass transition temperature of acrylic matrix is influenced mainly by increasing content of the filler.

Contrary to previous literature, introduction of compatibilizing additive (AAPTMA) does not cause a serious drop in glass transition temperature. [17] Mülhaupt et al. reported that introduction of 10 wt. % of montmorillonite and appropriate amount of compatibilizer (10 wt. % of lauryl methacrylate comonomer) causes a decrease in T_g from 110°C down to 80 °C, which gives ΔT_g = -30K. In our case, ΔT_g is lower and approximates just -13 K for co(E)-3,3/M 97,5/2,5 and 10 K for co(S)-4,4/M 90/10 (cf. Fig. 4). This indicates that, from practical point of view, the presented synthetic route utilizing AAPTMA as the compatibilizing agent is advantageous over the methods reported in ref. [17] where lauryl methacrylate was used as a compatibilizer.

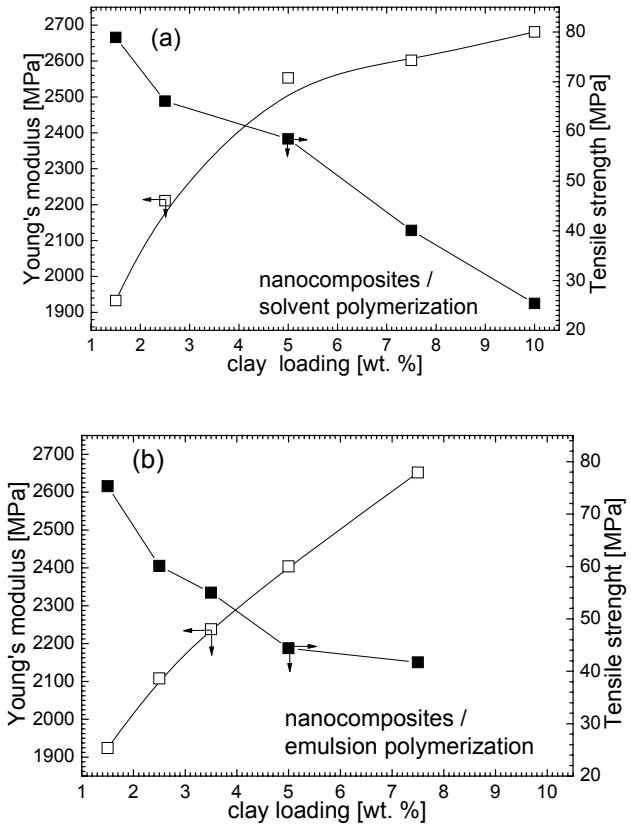

Fig. 5. Young's moduli and tensile strength of the nanocomposites obtained by solution polymerization (a) and emulsion polymerization (b) methods. Hollow squares (▫)– Young's modulus, solid squares (▪) – tensile strength.

Mechanical properties of obtained materials were evaluated by standard tensile tests. Figures 5 a – b show the Young's moduli and tensile strengths recorded for the nanocomposites loaded with different amounts of montmorillonite. Basically, the observations for solvent- and emulsion-polymerized nanocomposites are similar. Increasing loading of the clay in the nanocomposites causes gradual increase in Young's modulus. The stress at break, which is the ultimate strength that the material can sustain before breaking, however decreases with increasing silicate content. Below 5 wt. % of the filler, tensile strength remains at acceptable level but increasing

the clay content beyond this threshold causes further degradation of the mechanical performance. Even though the decrease in the tensile strength seems to be general problem in synthesizing the nanocomposites, without a detailed investigation on particular materials, it is impossible to explain clearly why the drop occurs. [18,19] This study however, was out of the scope of the current work.

Conclusions

Nanocomposites of acrylic polymers and montmorillonite were successfully synthesized via emulsion- and solution polymerization. Both presented methods allowed skipping of the usual sequence of preparation of the silicate for the purpose of formation of nanocomposites, which means that organophilization, drying, milling, etc. were redundant here. The emulsion polymerization was possible as acrylamide derivatives are more soluble in water in comparison to acrylic polymers. The report clearly shows that, in this case, the emulsion polymerization is advantageous method for synthesizing nanocomposites. In comparison to polymerization in solvent, it allowed more effective deflocculating and intercalating of the clay with acrylic polymers. The nanocomposites obtained by emulsion polymerization had clearly better thermal stability than materials synthesized in solution. In the case of 'emulsion nanocomposite', loaded with 5 wt. % of the clay, the temperature of 10 % of weight loss was by approximately 50 K higher than the one measured for neat poly(methyl methacrylate) (274°C and 225°C respectively). Independent of the route, the presence of small quantities of layered silicate in the composites causes substantial increase in stiffness of obtained materials. At the same time however, a decrease in the tensile strength was observed. Thus, the future research will be aimed at improving the mechanical performance of acrylic nanocomposites obtained by the methods described in this paper.

Experimental Part

Materials

Prior to polymerization, methyl methacrylate (MMA; 99%, Fluka) was purged with 5 wt. % solution of NaOH in water to remove stabilizer (hydroquinone). (3-acrylamidepropyl) trimethylammonium chloride (AAPTMA; 75 wt. % solution in water) was used as received from Aldrich. Benzoyl peroxide (BPO; 98%, Fluka) and potassium persulfate (pure, Sigma-Aldrich) were used as initiators in solution polymerization and emulsion polymerization respectively. The initiators were applied without purification. Synthetic sodium montmorillonite SOMASIF® ME100 (M) with cation exchange capacity - CEC - in a range of 0,7 – 0,8 meq/g, is produced by CO-OP Chemical, Japan. Main components of this silicate are: Si – 26,5 wt. %, Mg – 15,6 wt. %, Na – 4,1 wt. %, F – 3,8 wt. % Al. – 0,2 wt. %, Fe – 0,1 wt. %, the rest is oxygen. Solvents: tetrahydrofurane (THF) and methanol (MeOH) used in the study were supplied by Polish Chemical Reagents (POCh). Mersolan is a trade name of emulsion stabilizer produced by Rokita / Poland. Aluminum chloride ($AlCl_3$**,** pure) used as emulsion coagulation agent was purchased from Polish Chemical Reagents (POCh).

Preparation of nanocomposites

The materials were obtained through solution and emulsion polymerizations. In order to prepare the nanocomposites with different polymer/filler weight ratios, the amounts

of reagents used varied in particular cases. However, in all the systems, the 2,7:1 mole ratio between AAPTMA and CEC of montmorillonite was maintained. The compositions of resulting materials are listed in Table 1. Exemplary synthetic procedures are briefly described below.

Tab. 1. Abbreviations and compositions of obtained acrylic nanocomposites. First column (1*) indicates polymerization method. S = solution polymerization, E = emulsion polymerization.

1*	sample	filler	system components		molecular weight		
		M [wt. %]	AAPTMA [wt. %]	MMA [wt. %]	$\bar{M}_w \times 10^{-3}$	$\bar{M}_n \times 10^{-3}$	M_w/M_n
S	co(S)-0,5/M 98,5/1,5	1,5	0,5	98,0	190	79	2,4
	co(S)-1,1/M 97,5/2,5	2,5	1,1	96,4	187	78	2,4
	co(S)-2,2/M 95/5	5,0	2,2	92,8	182	79	2,3
	co(S)-3,3/M 92,5/7,5	7,5	3,3	89,2	187	72	2,6
	co(S)-4,4/M 90/10	10,0	4,4	85,6	162	58	2,8
E	co(E)-0,5/M 98,5/1,5	1,5	0,5	98,0	270	104	2,6
	co(E)-1,1/M 97,5/2,5	2,5	1,1	96,4	273	101	2,7
	co(E)-1,5/M 96,5/3,5	3,5	1,54	95,0	257	95	2,7
	co(E)-2,2/M 95/5	5,0	2,2	92,8	232	83	2,8
	co(E)-3,3/M 92,5/7,5	7,5	3,3	89,2	238	85	2,8

Solution polymerization

Five grams of montmorillonite (M; approx. 3,8 meq) was mixed with 2,2 g (10,6 mmol) AAPTMA and water (7,0 g) in a reactor vessel to form a viscous suspension (paste) and left overnight at room temperature to assure complete swelling of the clay. Then the paste was mixed with 210 g of a solvent (THF + MeOH; 2:1 weight ratio) and methyl methacrylate (MMA; 92,8 g; 0,93 mol). Finally, the initiator was added, the reactor was closed (BPO; 0,4 g; 1,7 mmol) and the system was refluxed (64°C) with continuous stirring under nitrogen atmosphere. After 3 hours, second portion of BPO (0,17 g; 0,7 mmol) was added, and the system was heated for additional 9 hours. When the polymerization was finished, the reactor was cooled down to room temperature, and the polymeric material was recovered by solvent evaporation. Resulting composite foil was dried at 50°C in ambient atmosphere followed by drying in vacuum (50°C) until constant mass was reached. The sample was abbreviated as co(S)-2,2/M 95/5 (see Tab. 1. for details).

Emulsion polymerization

5,0 g of montmorillonite was dispersed in 300 ml of water and vigorously stirred in three-necked flask at room temperature for 12 hours. After the time, 2,2 g of AAPTMA was added and the suspension was mixed for additional 12 h. Then, MMA (92,8 g; 0,93 mmol); emulsion stabilizer (Mersolan; 7,0 g) and potassium persulfate

(0,42g / 1,55 mmol dissolved in 50 ml of water) were simultaneously charged into reaction vessel and vigorously stirred. The polymerization was carried out at 75°C for 5 hours under nitrogen atmosphere. The emulsion was coagulated with $AlCl_3$ (10 wt. %, solution in water) followed by repeated washings of the dispersion with distilled water to remove any excess of aluminum chloride. Then, the product was filtered, air-dried and finally vacuum-dried at 50°C until constant weight was achieved.

GPC

Polymer average molecular weights and molecular weight distributions were estimated from gel-permeation chromatography (GPC) performed at room temperature in THF, freshly distilled over potassium, using apparatus equipped with Knauer HPLC-pump 64, styragel (Macherey & Nagel) columns and refractive index detector. Retention times were converted to polymer molecular weights using a universal calibration curve built from narrow molecular weight distribution poly(methyl methacrylate) standards. Obtained raw results were processed automatically using PSS WinGPC scientific v. 4.02 software. Since GPC analysis demands samples without solid additives, montmorillonite was removed from polymer samples by dissolving in THF followed by centrifugation at 3000 rpm for 15 min.

Processing

The samples obtained either by solvent or emulsion polymerizations were melted in an internal mixer with counter-rotating rotors for 2 minutes at 195°C and then mold-pressed for two minutes at temperature of 190°C and pressure 30 MPa. Resulting plates, were cut in bars with dimensions of 80 mm × 10 mm ×1 (±0,05) mm, appropriate to mechanical characterization. The samples for x-ray diffraction measurements had dimensions of 1 mm × 1 mm × 0,6 (± 0,1) mm.

Structural characterization

Powder X-ray diffraction measurements (XRD) were performed on a Siemens D500 θ-θ diffractometer fitted with a Cu X-ray tube operated at 35 kV /30 mA. Data was collected in step-scan mode within a scan range of 2θ from 1° to 10° in 0.05°/θ steps with an integration time of 5s per data point. Scanning electron micrographs were taken using JEOL 5800 LV SEM microscope.

Thermal analysis

Thermogravimetric measurements were carried out using Q-derivatograph (Paulik-Erdey system, Hungary) in order to evaluate thermal stability of obtained samples. The composites were heated in air atmosphere from room temperature up to 600°C at a heating rate of 10 K/min.

Differential scanning calorimetry

A differential scanning calorimeter (Mettler-Toledo DSC 821) was used to estimate glass transition temperature (T_g) of the nanocomposites. The measurements have been executed as follows – after fitting the samples to the same thermal history, they were heated from 25°C to 160°C at heating rate 10.0 K/min. T_g was evaluated from an inflection point on the curve recorded during heating, using the Mettler-Toledo Star^e software working on SunOS 5.5.1/x86 platform.

Mechanical testing

Tensile tests were performed using standard testing machine TIRA*test* 2705 manufactured by Tira Maschinenbau / Germany. Young's moduli and tensile strengths were measured in ambient conditions for at least five samples and than the average values were calculated.

Acknowledgements

The financial support through a grant 4 T09B 026 25 funded by KBN (Komitet Badan Naukowych) is gratefully acknowledged by the authors. We thank Prof. Dr. Jochen Gutmann of Max Planck Institute for Polymer Research / Mainz for his help with XRD measurements.

References

1. Ray, S.S.; Okamoto, M.; *Prog. Polym. Sci.* **2003**, 28, 1539.
2. Alexandre, M.; Dubois, P.; *Mater. Sci. Eng. A.* **2000**, 28, 1.
3. Tsipursky, S.I.; Drits; V.A.; *Clay Minerals* **1984**, 19, 177.
4. Ogata, N.; Kawakage, S.; Ogihara, T.; *J. Appl. Polym. Sci.* **1997**, 66, 573.
5. Weimer, M.W.; Chen, H.; Giannelis, E.P.; Sogah, D.Y.; *J. Am. Chem. Soc.* **1999**, 121, 1615.
6. Kiersnowski, A.; Dabrowski, P.; Budde, H.; Kressler, J.; Piglowski J.; *Eur. Polym. J.* **2004**, 40, 2591.
7. Xie, W.; Hwu, J.M.; Yiang, G.J.; Buthelezi, T.M.; Pan, W.P.; *Polym. Eng. Sci.* **2003**, 43, 214.
8. Tsen, C.R.; Wu, J.Y.; Lee, H.Y.; Chang, F.C.; *Polymer* **2001**, 42, 10063.
9. Noh, M.W.; Lee, D.C.; *Polym. Bull.* **1999**, 42, 619.
10. Reichert, P.; Nitz, H.; Klinke, S.; Brandtsch, R.; Thomann, R.; Mülhaupt, R.; *Macromol. Mater. Eng.* **2000**, 275, 8.
11. Kiersnowski, A.; Chamczynska, J.; Trelinska-Wlazlak, M.; Piglowski J.; *e-Polymers* **2005**, P_008, 1 (conference paper, *Intl. Polymer Seminar, Gliwice-Poland, 2005).*
12. Lvov, Y.; Ariga, K.; Ichinose, K.; Kunitake, I.; *Langmuir* **1996**, 12, 3038.
13. Zhu, J.; Start, P.; Mauritz, K.; Wilkie, C.; *Polymer Degradation and Stability* **2002**, 77, 253.
14. Biasci, L.; Aglietto, M.; Ruggeri, G.; Ciardelli, F.; *Polymer* **1994**, 35, 3296.
15. Pramoda, K.P.; Liu, T.; Liu, Z.; He, C.; Sue, H.-J.; *Polymer Degradation and Stability* **2003**, 81, 47.
16. Tabtiang, A.; Lumlong, S.; Venables, R.; *Eur. Polym. J.* **2000**, 36, 2559.
17. Dietsche, F.; Thomann, Y.; Thomann, R.; Mülhaupt, R.; *J. Appl. Polym. Sci.* **2000**, 75, 396.
18. Zeng, X.; Wilkie, C.A.; *Polymer Degradation and Stability* **2003**, 82, 441.
19. Kiersnowski, A.; Pigłowski, J.; *Eur. Polym. J.* **2004**, 40, 1199.